Assembly and force measurement with SPM-like probes in holographic optical tweezers

2009 New J. Phys. 11 023012

(http://iopscience.iop.org/1367-2630/11/2/023012)

New Journal of Physics
The open-access journal for physics

Assembly and force measurement with SPM-like probes in holographic optical tweezers

L Ikin[1], D M Carberry[1], G M Gibson[2], M J Padgett[2] and M J Miles[1]

[1] H H Wills Physics Laboratories, University of Bristol, Bristol, UK
[2] SUPA, Department of Physics and Astronomy, University of Glasgow, Glasgow, UK
E-mail: david.carberry@bristol.ac.uk and m.j.miles@bristol.ac.uk

New Journal of Physics **11** (2009) 023012 (8pp)
Received 30 October 2008
Published 6 February 2009
Online at http://www.njp.org/
doi:10.1088/1367-2630/11/2/023012

Abstract. In this paper we demonstrate the optical assembly and control of scanning probe microscopy (SPM)-like probes, using holographic optical tweezers. The probes are formed from cadmium sulphide rods and silica microspheres, the latter providing explicit trapping handles. Calibration of the trap stiffness allows us to use a precise measure of probe displacement to calculate the applied forces. We demonstrate that the optically controlled probe can exert a force in excess of 60 pN, over an area of 1×10^{-13} m^2, with a force sensitivity of 50 fN. We believe that probes similar to the ones presented here will have applications as nanotools in probing laser-sensitive cells/materials.

Contents

1. Introduction

Scanning probe microscopy (SPM) has been used as a tool to investigate various materials and their properties in numerous laboratories around the world with great success. It has been used to image surfaces with sub-nanometre resolution [1], map the location of receptor sites of various cells [2], characterize the deformability of cells [3] and stretch various polymers [4]–[6]. However, despite having been used for over 25 years, atomic force microscopes (AFMs) suffer from some potential shortfalls: they can only operate on objects that are adsorbed or bonded to a surface, and they typically scan only in one plane at a time. Forces are usually measured perpendicular or parallel to the cantilever's tip, and not in arbitrary directions. The cantilever can be modified to scan along the side of a waveguide or cell [7], but true three-dimensional (3D) force measurement has not yet been realized.

In a similar vein, optical tweezers have often been used to investigate a variety of materials. Examples include the stretching of DNA [8], manipulating sub-cellular organelles [9], accurately placing nanorods across metallic contacts [10], positioning microspheres into photonic crystal template structures [11], measuring the Raman spectra of trapped particles [12] and monitoring mechanotransduction within living cells [13]. One of the key benefits of optical tweezers over many other force measurement techniques is that optical microscopy can be used at the same time as force measurement, ensuring that the desired area of the sample is being investigated. Additionally, by integrating spatial light modulators into the optical tweezers [14]–[16], full 3D control of an arbitrary number of probe particles has become possible [17].

While microspheres are typically used as probes in optical tweezers [18, 19], some groups have investigated the use of lithographic or two-photon polymerization as potential probes [20]. Nanorods, with their small diameters and large length, could also act as useful probes. Several groups have already demonstrated control over optically trapped nanorods, whether they have been held vertically [19, 21] or parallel to the focal plane [10, 22]. A large amount of literature is already available in the SPM community to this effect, where nanotubes have been attached to SPM cantilever tips [23, 24]. However, as the dimensions of the nanorods are typically larger than that of a standard cantilever tip, they are typically only used for applications where the high aspect ratios of the nanorod are required.

When performing force measurements with optical tweezers one of two scenarios typically arises, and a choice must be made about which experimental route will be taken. To minimize the interaction areas nano-sized probes are used, but the low optical trapping constants of these particles results in large Brownian fluctuations and less positional control. Alternatively, if the Brownian motion needs to be minimized for greater positional control, larger microspheres are required—but the exact area of interaction becomes less well defined. In this paper we demonstrate a method to make use of the positional accuracy possible with large microspheres and the low interaction areas achievable with nanorods. This is demonstrated by assembling an SPM-like probe with our holographic optical tweezers, using microspheres as handles to fully control a nanorod in 3D control, followed by the realtime exertion and calculation of forces on the probe.

2. Experimental details

2.1. Equipment

As previously described [25] our holographic optical tweezers are based on an inverted microscope (Axiovert 200, Zeiss) with a 1.3 NA, 100× objective (Plan-Neofluor, Zeiss) and a motorized *xyz* stage (MS-2000, ASI). The trapping beam is provided by a titanium–sapphire laser (Coherent 899), pumped by a solid state laser (Verdi-V18, Coherent), emitting up to 4 W at 800 nm. The beam is expanded to fill an optically addressed SLM (X8267-14DB, Hamamatsu) and imaged onto the back aperture of the objective lens. The beam enters the microscope through the bottom port, a half waveplate and polarizing beamsplitter passes the titanium–sapphire laser while reflecting the illumination light onto a high-speed camera utilizing on-camera particle tracking (microCam-640, Durham Smart Imaging) [26, 27]. The on-board tracking uses a centre-of-mass algorithm to locate the average position of a microsphere within a defined region-of-interest, and passes only the coordinates of each object back to a controlling computer. The user can then continuously record the position of particles relative to the centre of the optical trap at kHz rates, substantially faster than traditional video tracking techniques. In this work the position of the microspheres attached to the probe were monitored at 2.5 kHz.

2.2. CdS nanowire synthesis

Following the method presented in [28, 29] single-crystal (100) silicon wafers were placed in an Edwards evaporator and coated with a 10 nm layer of gold. These wafers were then washed in ethanol, dried in air and transferred into a quartz tube. CdS powder (217921, Sigma-Aldrich) was placed in a ceramic boat inside the tube, and the entire assembly was inserted into a furnace. The CdS powder was positioned in the most intense part of the furnace, and the gold-coated silicon wafer was placed 100 mm downstream from it. A flow of argon gas (70 $cm^3\,min^{-1}$) was applied to the tube for the duration of each run. The furnace was heated to a temperature of 830 °C and maintained at that temperature for 60 min. The furnace was then cooled quickly to room temperature and the wafer transferred to a clean facility. The resulting nanorods were separated from the silicon substrate by cleaving with a razor blade. The rods were suspended in dimethylformamide and biotinylated using standard biotinylation processes. Following this the biotinylated rods were transferred back into water.

2.3. Probe formation

Biotin-coated CdS rods and 2 μm streptavidin-coated silica microspheres were deposited in a sample chamber maintaining their high local concentrations [29]. A number of spheres were optically trapped and translated to a region of high rod concentration. Using two or three optical traps to confine the rods [30], as opposed to the line trapping methods previously reported in [10] or the array of optical traps reported in [31], we added the microspheres to the structure sequentially. The near-instant bonding of multiple biotin and streptavidin molecules formed a rigid structure and completed the probe. On occasions where only a single bond formed, the microsphere was observed to 'roll' on the surface of the rod until further molecules bonded. Typically this occurred within a few seconds. A step-by-step process showing the assembly of a probe is shown in figure 1; video footage is available from stacks.iop.org/NJP/11/023012/mmedia as media1.mov.

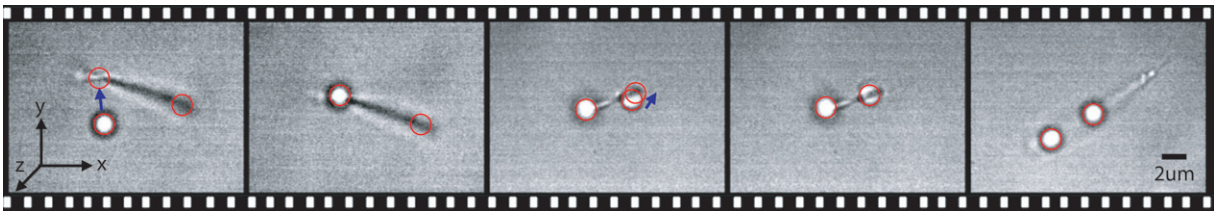

Figure 1. A typical probe is assembled in a step-by-step process. The 2 μm streptavidin-coated silica microspheres are sequentially brought into contact with the 300 nm diameter and 12 μm rod. The dotted red circles indicate the position of the optical traps; media1.mov (1.7 MB), available from stacks.iop.org/NJP/11/023012/mmedia, shows the assembly process more completely.

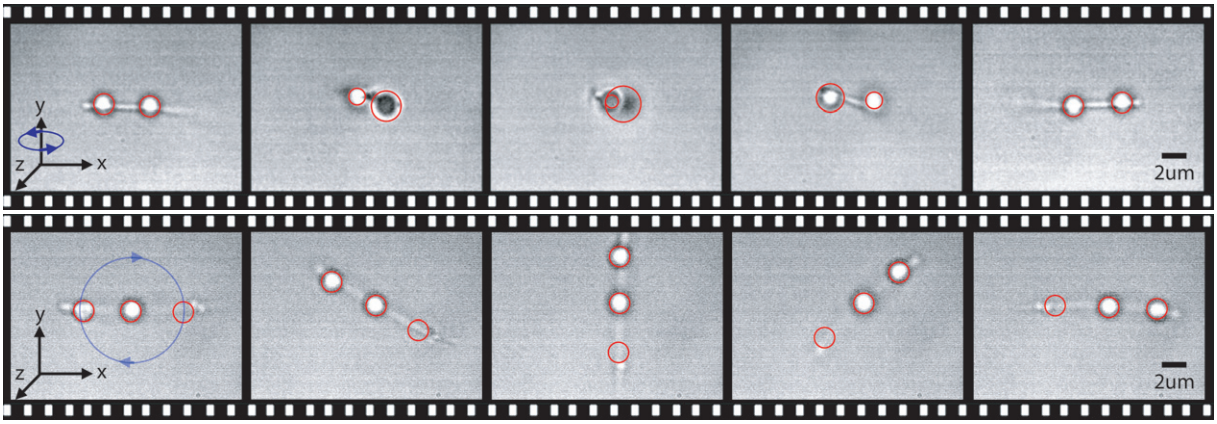

Figure 2. The probe is first rotated out of the focal plane, around the y-axis, by updating the hologram. The location of the trap centres is denoted by the red circles and the direction of rotation by the blue circle. The change in the diameter of the red trapping circles reflects the relative change to the height of the optical traps holding each microsphere. Secondly, an additional trap is added near the end of the probe to bring the nanorod into focus before rotating the probe in plane, around the z-axis. This can also be observed in media2.mov (3.4 MB), available from stacks.iop.org/NJP/11/023012/mmedia.

Following the assembly of the probe it was manipulated in 3D, as shown in figure 2. As the figure demonstrates, translations and rotations about arbitrary axes were simple to perform and control. The microsphere handles enabled the high refractive index nanorods ($n = 2.26$ at 800 nm) to be positioned at will. This type of probe is clearly capable of being used to investigate a variety of samples at arbitrary directions in space.

3. Force measurement

It is well known that the forces exerted on microspheres in an optical trap obey a Hookian force law. After the optical trapping constant, κ, has been determined the force can be calculated by simply multiplying it by the position of the microsphere relative to the centre of the optical trap. Typically, power spectrum density (PSD) analysis and/or equipartition are used to obtain

optical trapping constants in both the x-(horizontal) and y-(vertical) directions [32]. As the shape of the probe adds complexity to the PSD calculations, only equipartition was used to calibrate the trap; yielding trap constants of $\kappa_0 \equiv (\kappa_{0,x}, \kappa_{0,y}) = (4.72 \times 10^{-5}, 4.58 \times 10^{-5})$ N and $\kappa_1 = (4.77 \times 10^{-5}, 5.16 \times 10^{-5})$ N. To verify the calibration Stokes drag was employed. The stage was translated at a constant velocity of 12.75 μm s^{-1}, perpendicular to the long axis of the probe, while maintaining a constant hologram image to avoid artefacts caused by the discrete positioning of the optical traps between hologram updates [33]. Theory predicts that a translation of this velocity should result in force of $\approx 2.12 \times 10^{-12}$ N per sphere, which agrees within 10% with the measured average of 2.25×10^{-12} N. Between translations, when only thermal fluctuations will provide forces, the difference in consecutive forces was found to be 5.0×10^{-14} N, or 50 fN, 20 times more sensitive than most AFM techniques.

To demonstrate the ability to apply forces to materials the probe was brought into contact with a silicon shard, which had adsorbed to the surface of the sample chamber, numerous times. Continuous data and video were recorded during this process, media3.mov (available from stacks.iop.org/NJP/11/023012/mmedia) shows the process in its entirety. The stage was translated at 12.75 μm s^{-1} and each collision moved the probe to different distances relative to the shard, resulting in different applied forces. After the probe makes contact with the sample in the first collision it slightly rotates about its central point, between the trapped microspheres. This is seen as the difference in the signs of y_0 and y_1 traces in the force plots. In the second collision event the silicon shard 'catches' one of the nodules on the end of the nanorod and impedes the retraction of the probe. In collision 3, the probe tip initially slides on the sample, initially rotating the probe as in collision 1, but the total distance the probe is moved is increased further and the entire probe then moves in the y- and z-planes. Collision 4 shows the effect of further decreasing the distance between the optical traps and the silicon shard. In this case, the tip eventually slides around the shard and a minor catch is seen during the retraction. Collision 5 shows a smaller displacement of the stage and hence a lower applied force. There is virtually no y-movement in this case and all force is applied purely opposing the motion along the length of the rod. Collision 6 shows the effect of vastly reducing the optical trap–shard distance. The force exerted on the probe increases to such an extent that the probe almost completely defocuses in trap 0 before the probe slides around the shard. The small nodule observed approximately 1 μm from the tip catches on the shard during the retraction of the probe. In this case the probe was pulled from the optical trap and particle p0 ended up residing in trap 1, allowing the entire probe to rotate and be freed from the shard.

To emphasise the video more clearly, figure 3 displays three images from the 4th collision and a zoomed in section of the force profile. Similar detailed analyses could have been performed on any of the other probing events. The green dashed lines are used to illustrate the time and corresponding forces of each frame. The timelines on the charts have not been modified, maintaining the time relationship with the movie. In the first frame the probe had just made contact with the shard, and consequently no forces are observed. As time progresses an increasing amount of force is applied. The difference in the magnitude of the forces measured by x_0 and x_1 is a result of the changes in the focal plane of the microspheres (not measured). The relative intensity of x_0 and x_1 could be used to indicate the amount of z-defocusing and the consequent height of both microspheres. Between $t = 8.82$ s and 8.87 s the different sign of $F_{y,0}$ and $F_{y,1}$ indicates that the probe twists about a point between the two microspheres within the trapping plane. The second frame shows the displacement of each microsphere with respect to the optical trap centres, and defocusing of the entire probe can be observed. The force profile

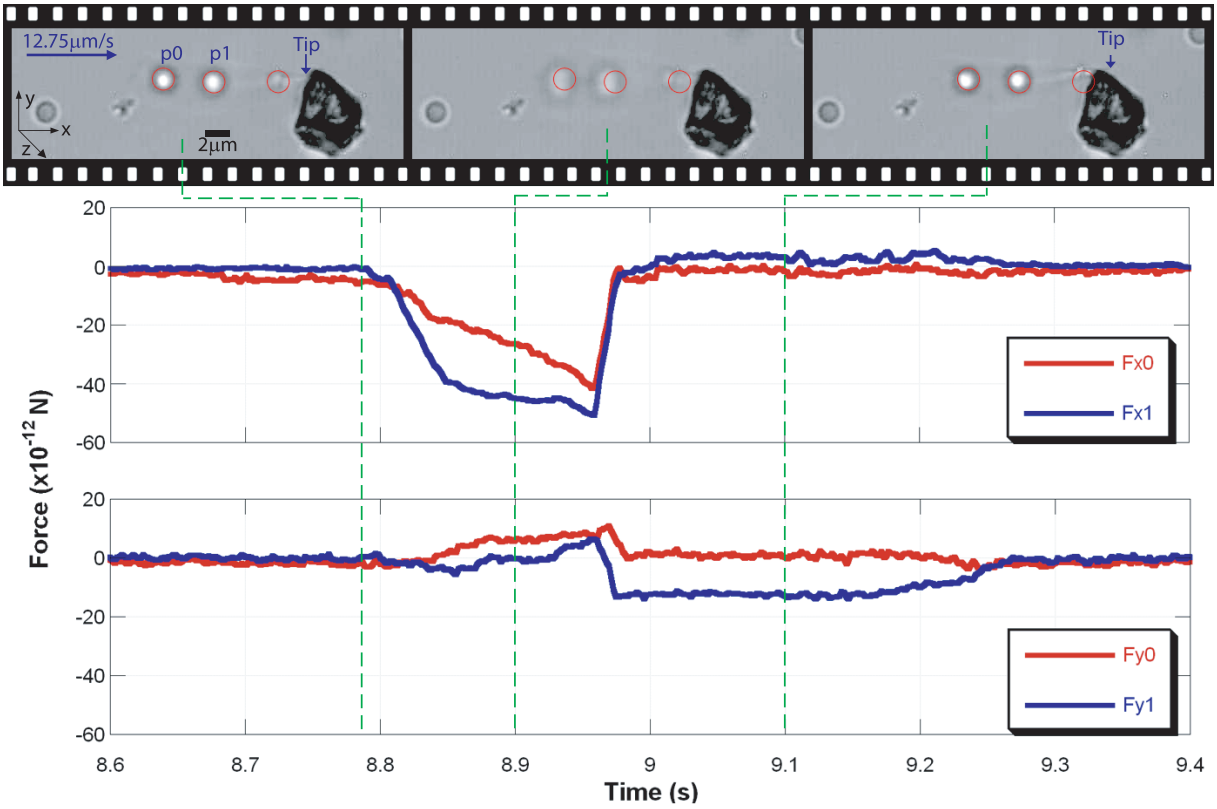

Figure 3. Three frames have been extracted from media3.mov (3.2 MB) and are shown with an expanded view of the applied forces. The green dashed lines indicate the time each frame is sampled. p0 and p1 refer to the locations of optical trap 0 and 1 (red circles), and also show the location of the centres of the microspheres attached to the nanorod. The stage was translated at 12.75 μm s^{-1}, until the probe collides with a silicon shard adhered to the surface (frame 1). The relative defocussing and torques can be calculated from the force profiles.

demonstrates that the entire probe shifts in the $+y$-direction at $t = 8.92$ s, enabling the probe to slip from its initial location at $t = 8.96$ s and slide around the point of the shard. A torque event is clearly present by inspection of the movie and the y force profiles. Frame 3 of figure 3 shows the tip protruding past the top of the shard. Forces $F_{x,0}$, $F_{x,1}$ and $F_{y,0}$ return to near zero force, and only the forces rotating the probe are seen in $F_{y,1}$. At this point in time the user reversed the direction of the probe, resulting in the observed plateau and reduction of torque.

4. Conclusions

SPM-like probes have been assembled from steptavidin-coated silica microspheres and biotin-coated CdS rods. In the future the tips of such rods could be functionalized. The range of forces that these probes can exert on an external structure have been demonstrated to range from 50 fN to in excess of 60 pN. While the extent of the residual Brownian motion means that the technique is unlikely to result in the same levels of positional control capable with current SPM systems, this proof of principle study demonstrates potential uses of optically trapped probes within

liquid media, compatible with biological systems. In particular, this type of probe could be used to investigate a living cell in true environmental conditions, something that will challenge traditional SPMs.

Acknowledgment

This project is funded by a Basic Technology Grant through the Research Councils of the United Kingdom.

References

[1] Baker A A, Helbert W, Sugiyama J and Miles M J 1997 High-resolution atomic force microscopy of native valonia cellulose I microcrystals *J. Struct. Biol.* **119** 129–38
[2] Grandbois M, Dettmann W, Benoit M and Gaub H E 2000 Affinity imaging of red blood cells using an atomic force microscope *J. Histochem. Cytochem.* **48** 719–24
[3] Chtcheglova L A, Waschke J, Wildling L, Drenckhahn D and Hinterdorfer P 2007 Nano-scale dynamic recognition imaging on vascular endothelial cells *Biophys. J.* **93** L11–3
[4] Florin E L, Moy V T and Gaub H E 1994 Adhesion forces between individual ligand-receptor pairs *Science* **264** 415–7
[5] Humphris A D L, Tamayo J and Miles M J 2000 Active quality factor control in liquids for force spectroscopy *Langmuir* **16** 7891–4
[6] Haupt B J, Senden T J and Sevick E M 2002 AFM Evidence of Rayleigh instability in single polymer chains *Langmuir* **18** 2174–82
[7] Dai G, Wolff H, Pohlenz F, Danzebrink H-U and Wilkening G 2006 Atomic force probe for sidewall scanning of nano- and microstructures *Appl. Phys. Lett.* **88** 171908
[8] Bustamante C, Smith S B, Liphardt J and Smith D 2000 Single-molecule studies of DNA mechanics *Curr. Opin. Struct. Biol.* **10** 279–85
[9] Ashkin A and Dziedzic J M 1989 Internal cell manipulation using infrared laser traps *Proc. Natl Acad. Sci. USA* **86** 7914–8
[10] Yu T, Cheong F-C and Sow C-H 2004 The manipulation and assembly of CuO nanorods with line optical tweezers *Nanotechnology* **15** 1732–6
[11] Benito D C, Carberry D M, Simpson S H, Gibson G M, Padgett M J, Rarity J G, Miles M J and Hanna S 2008 Constructing 3D crystal templates for photonic band gap materials using holographic optical tweezers *Opt. Express* **16** 13005–15
[12] Jordan P, Cooper J, McNay G, Docherty F, Graham D, Smith W, Sinclair G and Padgett M J 2005 Surface-enhanced resonance Raman scattering in optical tweezers using co-axial second harmonic generation *Opt. Express* **13** 4148
[13] Wang Y, Botvinick E L, Zhao Y, Berns M W, Usami S, Tsien R Y and Chien S 2005 Visualizing the mechanical activation of src *Nature* **434** 1040–5
[14] Reicherter M, Haist T, Wagemann E U and Tiziani H J 1999 Optical particle trapping with computer-generated holograms written on a liquid-crystal display *Opt. Lett.* **24** 608–10
[15] Curtis J E, Koss B A and Grier D G 2002 Dynamic holographic optical tweezers *Opt. Commun.* **207** 169–75
[16] Simpson S H and Hanna S 2006 Numerical calculation of interparticle forces arising in association with holographic assembly *J. Opt. Soc. Am.* A **23** 1419–31
[17] Sinclair G, Jordan P, Courtial J, Padgett M J, Cooper J and Laczik Z 2004 Assembly of 3-dimensional structures using programmable holographic optical tweezers *Opt. Express* **12** 5475–80
[18] Friese M E J, Truscott A G, Rubinsztein-Dunlop H and Heckenberg N R 1999 Three-dimensional imaging with optical tweezers *Appl. Opt.* **38** 6597–6603

[19] Ghislain L P and Webb W W 1993 Scanning-force microscope based on an optical trap *Opt. Lett.* **18** 1678
[20] Rodrigo P J, Gammelgaard L, Bøggild P, Perch-Nielsen I and Glückstad J 2005 Actuation of microfabricated tools using multiple GPC-based counterpropagating-beam traps *Opt. Express* **13** 6899–904
[21] Pauzauskie P J, Radenovic A, Trepagnier E, Shroff H, Yang P and Liphardt J 2006 Optical trapping and integration of semiconductor nanowire assemblies in water *Nat. Mater.* **5** 97–101
[22] van der Horst A, Campbell A I, van Vugt L K, Vanmaekelbergh D A, Dogterom M and van Blaaderen A 2007 Manipulating metal-oxide nanowires using counter-propagating optical line tweezers *Opt. Express* **15** 11629–39
[23] Dai H, Hafner J H, Rinzler A G, Colbert D T and Smalley R E 1996 Nanotubes as nanoprobes in scanning probe microscopy *Nature* **384** 147–50
[24] Seo J W, Couteau E, Umek P, Hernadi K, Marcoux P, Lukic B, Miko Cs, Milas M, Gaal R and Forro L 2003 Synthesis and manipulation of carbon nanotubes *New J. Phys.* **5** 120
[25] Gibson G, Carberry D M, Whyte G, Leach J, Courtial J, Jackson J C, Robert D J, Miles M J and Padgett M 2008 Holographic assembly workstation for optical manipulation *J. Opt. A: Pure Appl. Opt.* **10** 044009
[26] Saunter C D, Love G D, Johns M and Holmes J 2005 FPGA technology for high speed, low cost adaptive optics—art. no. 61081g *5th International Workshop on Adaptive Optics for Industry and Medicine, Beijing, Peoples Republic of China* ed W H Jiang p 429
[27] Di Leonardo R, Keen S, Leach J, Saunter C D, Love G D, Ruocco G and Padgett M J 2007 Eigenmodes of a hydrodynamically coupled micron-size multiple-particle ring *Phys. Rev.* E **76** 061402
[28] Ma R M, Wei X L, Dai L, Huo H B and Qin G G 2007 Synthesis of CdS nanowire networks and their optical and electrical properties *Nanotechnology* **18** 205605
[29] Ikin L, Carberry D M, Grieve J A, Gibson G M, Padgett M J and Miles M J 2008 Construction and manipulation of structures using optical tweezers *SPIE Optics and Photonics* (San Diego, CA: SPIE)
[30] Benito D C, Simpson S H and Hanna S 2008 FDTD simulations of forces on particles during holographic assembly *Opt. Express* **16** 2942–57
[31] Agarwal R, Ladavac K, Roichman Y, Yu G, Lieber C M and Grier D G 2005 Manipulation and assembly of nanowires with holographic optical traps *Opt. Express* **13** 8906–12
[32] Gibson G M, Leach J, Keen S, Wright A J and Padgett M J 2008 Measuring the accuracy of particle position and force in optical tweezers using high-speed video microscopy *Opt. Express* **16** 14561–70
[33] Eriksson E, Keen S, Leach J, Goksör M and Padgett M J 2007 The effect of external forces on discrete motion within holographic optical tweezers *Opt. Express* **15** 18268–74